Contents lists available at ScienceDirect

Materials Science & Engineering C

journal homepage: www.elsevier.com

Nanostructured lipid dispersions for topical administration of crocin, a potent antioxidant from saffron (*Crocus sativus* L.)

Elisabetta Esposito [a, *], Markus Drechsler [b], Paolo Mariani [c], Anna Maria Panico [d], Venera Cardile [e], Lucia Crascì [d], Federica Carducci [c], Adriana Carol Eleonora Graziano [e], Rita Cortesi [a, *], Carmelo Puglia [d]

[a] *Department of Life Sciences and Biotechnology, University of Ferrara, I-44121 Ferrara, Italy*
[b] *Macromolecular Chemistry II, University of Bayreuth, Germany*
[c] *Department of Life and Environmental Sciences, Università Politecnica delle Marche, I-60131 Ancona, Italy*
[d] *Department of Drug Sciences, University of Catania, I-95125 Catania, Italy*
[e] *Department of Biomedical Sciences, University of Catania, I-95125 Catania, Italy*

ARTICLE INFO

Article history:
Received 27 July 2016
Received in revised form 13 September 2016
Accepted 23 October 2016
Available online xxx

Keywords:
Nanotechnology
Materials science
Chemical stability
Formulation
Antioxidant

ABSTRACT

Crocin, a potent antioxidant obtained from saffron, shows anticancer activity in in vivo models. Unfortunately unfavorable physicochemical features compromise its use in topical therapy.

The present study describes the preparation and characterization of nanostructured lipid dispersions as drug delivery systems for topical administration of crocin and the evaluation of antioxidant and antiproliferative effects of crocin once encapsulated into nanostructured lipid dispersions.

Nanostructured lipid dispersions based on monoolein in mixture with sodium cholate and sodium caseinate have been characterized by cryo-TEM and PCS. Crocin permeation was evaluated in vitro by Franz cells, while the oxygen radical absorbance capacity assay was used to evaluate the antioxidant activity. Furthermore, the antiproliferative activity was tested in vitro by the MTT test using a human melanoma cell line.

The emulsification of monoolein with sodium cholate and sodium caseinate led to dispersions of cubosomes, hexasomes, sponge systems and vesicles, depending on the employed emulsifiers. Permeation and shelf life studies demonstrated that nanostructured lipid dispersions enabled to control both rate of crocin diffusion through the skin and crocin degradation. The oxygen radical absorbance capacity assay pointed out an interesting and prolonged antioxidant activity of crocin while the MTT test showed an increase of crocin cytotoxic effect after incorporation in nanostructured lipid dispersions.

This work has highlighted that nanostructured lipid dispersions can protect the labile molecule crocin from degradation, control its skin diffusion and prolong antioxidant activity, therefore suggesting the suitability of nanostructured lipid dispersions for crocin topical administration.

1. Introduction

In the last few years researchers have been focusing on the health benefits of the constituent of Mediterranean diet, in particular the spice saffron has been evaluated for its unique and numerous therapeutic properties. Apart from its long historical use in many specialty dishes, saffron has been used to treat a wide variety of human health conditions [1]. Saffron consists of the dried dark red or yellow "stigmas" of the crocus flower, *Crocus sativus* L. In particular, studies have been conducted on the biological and pharmacological properties of two saffron components, safranal and crocin (CRO) [2]. CRO, the digentiobiosyl ester of crocetin, is one of the few water soluble carotenoids found in nature. CRO is a potent antioxidant with antiapoptotic action, antidepressant and aphrodisiac properties, it displays therapeutic efficacy on many organs, including the nervous, gastrointestinal, cardiovascular, genital, endocrine and immune systems. In addition, in multiple studies, scientists have been finding that saffron has the unique ability to both slow and reverse cancer growth [3–5]. The cancer-preventive properties of saffron consist of inhibiting the promotion of tumors and preventing chemical modifications to DNA that can activate cancer genes or induce new cancer-causing mutations. In particular it has been demonstrated an inhibitory effect of CRO on skin-tumor promotion in mice [6].

Human skin cells are continuously exposed to genotoxic stress, which may result in DNA damage. The carcinogenesis process in murine and possibly human skin is a multi step process involving the distinct phases of initiation, promotion and progression. The tumor initiation stage is an irreversible process in which carcinogens damage the DNA and induce mutations in critical genes in stem cells. On the contrary the process of promotion is reversible, providing a chance to interrupt or delay the development of altered lesions resulting in tumor formation, finally tumor progression is the process in which the growing tumor becomes more aggressive [7,8]. Several plant phenolic compounds, such as CRO, exhibit chemoprotective properties by hindering the different stages of multi step skin carcino-

Abbreviations: NLD, nanostructured lipid dispersions; CRO, crocin; cryo-TEM, Cryo-transmission electron microscopy; SCE, *Stratum Corneum Epidermis*; ORAC, oxygen radical absorbance capacity

* Corresponding authors.
Email addresses: ese@unife.it (E. Esposito); crt@unife.it (R. Cortesi)

http://dx.doi.org/10.1016/j.msec.2016.10.045
0928-4931/

genesis, especially tumor promotion [9]. Nonetheless the exact inhibitory mechanisms of CRO on tumor promotion are still unclear. The major limit to CRO use is its high instability to light, pH, temperature and oxygen [10]. To obtain a suitable vehicle for CRO, able to reduce its chemical degradation, in the present study we investigate the inclusion of CRO in nanostructured lipid dispersions (NLD). NLD generate from the self-assembly of amphiphilic lipids such as unsaturated long-chain monoglycerides, (e.g. monoolein) in water [11,12]. Notably, in NLD, the dispersion of monoglyceride gives rise to complex lyotropic liquid crystalline nanostructures like micellar, lamellar, hexagonal, and cubic phases. The choice of the emulsifier agent to be employed in association with monoolein influences both morphology and properties of the NLD [13]. NLD can be considered as advanced nano-vehicles able to solubilize hydrophilic and lipophilic molecules in a physiologic environment, controlling their delivery and protecting them from degradation.

The aim of this study is the preparation and characterization of CRO containing NLD intended for cutaneous administration to treat melanoma and skin inflammatory pathologies.

Firstly a formulation study was conducted, in particular, after NLD production by natural components, such as monoolein, sodium cholate and sodium caseinate, morphology and size distribution have been investigated.

Furthermore, to reproduce cutaneous administration, the in vitro diffusion kinetics of CRO from the different NLD have been compared by Franz cell coupled with excised human skin membranes [*Stratum Corneum Epidermis* (SCE)].

Finally CRO loaded NLD were studied in order to understand the influence of the vehicle on antioxidant properties and antiproliferative effect of CRO by oxygen radical absorbance capacity (ORAC) assay and MTT test respectively.

2. Experimental

2.1. Materials

Glyceryl monooleate RYLO MG 19 (monoolein) was a gift from Danisco Cultor (Grindsted, Denmark). Crocin (CRO) (crocetin digentibiose ester), sodium cholate (3α,7α,12α-Trihydroxy-5β-cholan-24-oic acid sodium salt), sodium caseinate (αS1, αS2, β, κ), fluorescein (FL), and AAPH (2,2′-azobis (2-methylpropionammide) dihydrochloride) were purchased from Sigma-Aldrich (St Louis, MO, USA). Solvents were of HPLC grade and all other chemicals were of analytical grade.

2.2. NLD preparation

Production of dispersions was based on the emulsification of monoolein (4.5% w/w) and emulsifier in bidistilled water at 70 °C [14]. The emulsifier was alternatively constituted by sodium cholate (0.15% w/w) in the case of NLD-A, or a mixture of sodium cholate (0.15% w/w) and sodium caseinate (0.07% w/w) in the case of NLD-B (Table 1). Throughout the manuscript the term "empty NLD" refers to NLD produced in the absence of CRO and "NLD" to CRO containing NLD.

After emulsification, the dispersions were subjected to homogenization (15,000 rev min^{-} 1, Ultra Turrax, Janke & Kunkel, Ika-Werk, Sardo, Italy) at 60 °C for 1 min, afterwards they were cooled.

In the case of CRO containing NLD, 50 mg of CRO (0.02% w/w with respect to the monoolein, 0.1% w/w with respect to the dispersion) was added to the molten monoolein/emulsifier mixture and dissolved before addition to the aqueous solution (Table 1). During production the vial was protected from light with an aluminum foil to prevent photodegradation of CRO.

Empty NLD and NLD were then filtered through a mixed esters cellulose membrane (0.6 μm pore size Whatman® membrane filters, Sigma-Aldrich, St Louis, MO, USA) in order to remove the possible presence of lipid aggregates. All glassware and filter employed for the NLD production were accurately weighted before and after preparation of NLD. The NLD dispersions were stored at room temperature in glass vials. Details on determination of aggregate recovery are reported in Supplementary Data. In vitro and ex-vivo studies have been performed on filtered NLD.

2.3. Characterization of nanostructured lipid dispersions

2.3.1. Cryo-transmission electron microscopy (cryo-TEM)

Samples were vitrified as described in a previous study [14]. The vitrified specimen was transferred to a Zeiss EM922Omega (Carl Zeiss Microscopy, Oberkochen, Germany) transmission electron microscope using a cryoholder (CT3500, Gatan, Munich, Germany). Sample temperature was kept below 100 K throughout the examination. Specimens were examined with reduced doses of about 1000–2000 e/nm^2 at 200 kV. Images were recorded by a CCD digital camera (Ultrascan 1000, Gatan, Munich, Germany) and analysed using a GMS 1.8 software (Gatan, Munich, Germany).

2.3.2. X-ray diffraction measurements

X-ray diffraction experiments were performed on NLD before filtration using a 3.5 kW Philips PW 1830 X-ray generator (Amsterdam, Netherlands) equipped with a Guinier-type focusing camera (home-made design and construction, Ancona, Italy) operating with a bent quartz crystal monochromator (λ = 1.54 Å). Diffraction patterns were recorded on GNR Analytical Instruments Imaging Plate system (Novara, Italy). The investigated Q-range ($Q = 4\pi \sin\theta / \lambda$, where 2θ is the scattering angle) was 0.02–0.35 $Å^{-1}$. Samples were held in a tight vacuum cylindrical cell provided with thin mylar windows. Diffraction data were collected at 35 °C. In each experiment, a number of Bragg peaks was detected in the low-angle region and the peak indexing was performed considering the different symmetries commonly observed in lipidic phases. Once derived the lattice symmetry, the unit cell dimension, a, was calculated from the averaged spacing of the observed peaks.

Table 1
Composition of NLD and structural organization obtained by X-ray diffraction experiments on NLD before filtration.

Formulation	Composition (% w/w)					Unit cell value (a), ± 1 Å	Morphology
	Monoolein	Sodium cholate	Sodium caseinate	Water	CRO		
Empty NLD-A	4.50	0.15	–	95.35	–	153.4 Å (cubic phase 229)	Cubosome
Empty NLD-B	4.50	0.15	0.07	95.28	–	151.7 Å (cubic phase 229)	Cubosome
NLD-A	4.50	0.15	–	95.25	0.1	148.3 Å (cubic phase 229)	Cubosome
NLD-B	4.50	0.15	0.07	95.18	0.1	56.9 Å (hexagonal phase)	Hexasome

2.3.3. 2.3.4 photon correlation spectroscopy (PCS)

Submicron particle size analysis was performed using a Zetasizer Nano Series, Nano SP90 (Malvern Instr., Malvern, England) equipped with a 5 mW helium neon laser with a wavelength output of 633 nm. Glassware was cleaned of dust by washing with detergent and rinsing twice with sterile water. Measurements were performed at 25 °C at an angle of 90° with a run time of at least 180 s. Samples were diluted with bidistilled water in a 1:50 v:v ratio. Data were analysed using the "CONTIN" method [15]. PCS analysis of the NLD dispersions as well as in vitro and in vivo experiments were performed after filtration, without taking into account the fraction of larger particles whose dimensions have been measured by laser diffraction (Horiba, LA-920, Horiba Ltd., Tokyo, Japan). Data were means of six determinations on different batches of the same type of dispersion.

2.4. Drug content of dispersions

The encapsulation efficiency (EE) and loading capacity (LC) were determined on filtered NLD as described by Nayak and colleagues [16]. One hundred microliter aliquot of each NLD batch was loaded in a centrifugal filter (Microcon centrifugal filter unit YM-10 membrane, NMWCO 10 kDa, Sigma Aldrich, St Louis, MO, USA) and centrifuged (Spectrafuge™ 24D Digital Microcentrifuge, Woodbridge NJ, USA) at 8000 rpm for 20 min. The amount of entrapped CRO was determined by dissolving the lipid phase in the supernatant with a known amount of ethanol (1:10, v/v), while the amount of free CRO was determined directly in the filtrate constituted of the aqueous phase. Supernatant and filtrate were analysed for CRO content by high performance liquid chromatography (HPLC), as below reported. The encapsulation parameters were determined as follows.

$$EE = L\ CRO/T\ CRO \times 100 \quad (1)$$

$$LC = L\ CRO/T\ LIPID \times 100 \quad (2)$$

where L CRO is the amount of drug encapsulated in NLD; T CRO and T LIPID are the total weight of CRO and of lipid used for the NLD preparation, respectively. All data were the mean of four determinations on 6 different batches of the same type of dispersion. Details on EE evaluation in aggregates are reported in Supplementary data.

Chemical stability was evaluated on filtered drug loaded formulations, stored at 25 °C in the dark for 3 months, determining CRO content by HPLC analyses.

2.5. In vitro percutaneous absorption studies

For in vitro diffusion studies, samples of adult human skin (mean age 36 ± 8 years) from breast reduction operations were employed. The epidermal membranes were dried in a desiccator at approximately 25% relative humidity (RH) and then stored in aluminum foil at 4 ± 1 °C until use. Preliminary experiments were carried out to assess SCE samples for barrier integrity by measuring the in vitro permeability of [3H] water through the membranes using the Franz cells described below. The value of the permeability coefficient (Pm) for tritiated water was found to be $1.6 \pm 0.2 \times 10^{-3}$ cm/h, which agreed well with those for tritiated water reported by others, using human SCE samples [17].

Twelve randomized samples of dried SCE were rehydrated by immersion in distilled water at room temperature for 1 h before being mounted in Franz-type diffusion cells supplied by Vetrotecnica (Padova, Italy).

The exposed skin surface area was 0.78 cm^2 (the diameter of the orifice was 1 cm). The receptor compartment contained 5 ml of phosphate buffer 60 mM pH 7.4. This solution was stirred with the help of a magnetic bar at 500 rpm and thermostated at 35 ± 1 °C during all the experiments.

Approximately 500 μl of each formulation was placed on the skin surface in the donor compartment and the latter was sealed with a cap to avoid evaporation. Samples (200 μl) of receptor phase were withdrawn at predetermined time intervals comprised between 1 and 24 h. CRO concentration in the receptor phase was measured using HPLC. Each removed sample was replaced with an equal volume of phosphate buffer. CRO concentration was determined four times in independent experiments and the mean values ± standard deviations were calculated.

The cumulative amount of drug penetrating the skin was plotted against time. The slope of the linear portion of the curve and the c-intercept values (lag time) were determined by linear regression analysis. The experimentally observed fluxes (μg/cm^2/h), at steady state, were calculated by dividing the slope of the linear portion of the curve by the area of the skin surface through which diffusion took place. Normalized fluxes were then calculated by dividing the observed fluxes by the CRO concentration (in mg/ml) in the analysed form.

2.6. HPLC procedure

HPLC determinations were performed using a quaternary pump (Agilent Technologies 1200 series, USA), an UV-detector operating at 440 nm and a 7125 Rheodyne injection valve with a 50 μl loop. Samples were loaded on a stainless steel C-18 reverse-phase column (15 × 0.46 cm) packed with 5 μm particles (Grace® - Alltima, Alltech, USA).

Elution was performed with a mobile phase containing methanol, water 65:35 v/v at a flow rate of 0.8 ml/min, retention time was 4–4.5 min. The method was validated for linearity ($R^2 = 0.995$), repeatability (relative standard deviation 0.01%, n = 6 injections) and limit of quantification (0.04 μg/ml).

2.7. Oxygen radical absorbance assay

An oxygen radical absorbance capacity (ORAC) assay was used to determine qualitatively the antioxidant activity of NLD-A and NLD-B [18]. A fresh solution of CRO (25 μl), empty and loaded vehicles (25 μl) were placed in 96-well tissue culture plates. 150 μl of Fluorescein (FL) (10 nM) was used as the probe to assess the antioxidant activity. 25 μl of water-soluble azo-compound AAPH (100 mM) was used as a radical initiator to generate free radicals at a constant rate. A positive control (FL solution containing AAPH), a negative control (FL solution containing no AAPH), CRO solution at the concentration used in NLD, empty NLD-A, empty NLD-B, NLD-A, NLD-A and NLD-B were run simultaneously in phosphate-buffered saline (PBS). A timer was started upon introduction of the free radical generator and the plate was stored in the dark at 37 °C. At each specified time point the fluorescence of the solution was measured (excitation 492 nm, emission 535 nm) using a Wallac 1420 Victor 3 96-well plate reader fluorimeter (Perkin Elmer, USA) and plotted as a function of time with Origin®7 software (Origin Lab Corporation).

The Y axis graph was split as follow: 10,000 to 16,000 RFU (Fig. 6A and B).

2.8. Biological experiments

2.8.1. Cell culture

The human melanoma cell line A375 was provided by American Type Culture Collection (Rockville, MD, USA). Cell line was cultured in Dulbecco's modified Eagle's medium (DMEM; Sigma-Aldrich, Milan, Italy) supplemented with 10% fetal bovine serum, (FBS, Invitrogen, Carlsbad, CA, USA), 4 mM L-glutamine, 4500 mg/l glucose, 1 mM sodium pyruvate, 1500 mg/l sodium bicarbonate, 100 U/ml penicillin and 100 μg/ml streptomycin. Primary lines of non-tumorigenic, non-immortalized, human adult fibroblasts were grown in Dulbecco's modified Eagle's medium containing 10% fetal calf serum, 100 U/ml penicillin, 100 μg/ml streptomycin, and 25 μg/ml fungizone (Invitrogen Life Technologies, Inc.).

Cells were incubated at 37 °C in a humidified atmosphere of 95% air/5% CO_2. A sub-cultivation ratio of 1:3 to 1:4 twice weekly was performed by using trypsin (0.25%)–EDTA (1 mM) for the detachment. The medium was changed every 2–3 days.

2.8.2. Cell treatments

One day before the experiments, cells were trypsinized, counted, and seeded at an initial density of 8×10^3 cells per microwell in flat-bottomed 96-wells culture microplates (Thermo Scientific Nunc, Milan, Italy) and incubated at 37 °C in a humidified atmosphere containing CO_2 (5%) with complete medium without FBS for 24 h. After that, the medium was removed and replaced with treatment medium containing CRO PBS solution, empty NLD-A, empty NLD-B, NLD-A, NLD-A or NLD-B (CRO 0.1% w/w) at dilution 1:100 v/v. After 72 h of incubation, cells proliferation was evaluated.

2.8.3. MTT test

Cell growth was tested by MTT assay, based on the conversion by mitochondrial dehydrogenases of a substrate containing a tetrazolium ring into blue formazan, detectable spectrophotometrically.

At the end of treatment time, the media were removed and a solution of 3-(4,5-dimethyl-thiazol-2-yl)2,5-diphenyl-tetrazolium bromide (0.5 mg/ml PBS) was added to each microwell. After 3 h of incubation at 37 °C, the supernatant was removed and replaced with DMSO (100 μl). The optical density was measured with a microplate spectrophotometer reader (Digital and Analog Systems, Rome, Italy) at $\lambda = 550$ nm. Each sample was tested in quadruplicate ($n = 12$) and cell viability was reported as percentage (%) compared to the controls (untreated, empty NLD-A or empty NLD-B treated cells, respectively).

2.9. Statistical analysis

Statistical analysis of data was performed using the Student's *t*-test. A probability $p < 0.05$ was considered significant in this study.

3. Results

3.1. Production and characterization of NLD

Two types of NLD have been produced, based on the use of monoolein associated to naturally derived materials, such as sodium cholate and sodium caseinate, employed as stabilizers. The use of sodium cholate resulted in the production of transparent dispersions (named NLD-A), while sodium caseinate together with sodium cholate enabled to produce opaque milky dispersions (named NLD-B).

After producing NLD the macroscopic appearance of the dispersions was evaluated. The only variation due to CRO presence was the change of colour dispersions from white to yellow. Few aggregates have been found in both NLD-A and NLD-B. Regarding the monoolein plus stabilizer weight before production, the aggregate weight ratio after filtration and desiccation was $5 \pm 0.7\%$ and $4.5 \pm 0.5\%$ for NLD-A and NLD-B respectively (Supplementary data).

Fig. 1 reports cryo-TEM images of empty NLD-A (A, B) and empty NLD-B (C, D) before (A, C) and after (B, D) filtration. The use of sodium cholate resulted in the formation of few cubic structures (Fig. 1A) and more abundant unilamellar vesicles (Fig. 1B), whereas the association of sodium cholate and sodium caseinate (NLD-B) led to the formation of a heterogeneous system constituted of huge cubic structures (Fig. 1C), uni-lamellar vesicles, bi-lamellar vesicles, invaginated vesicles and some sponge area (Fig. 1D). The cubic structures were not more detectable by cryo-TEM after sample filtration (B, D). The arrow in panel D indicates a sponge area. In order to disclose the effect of CRO on NLD morphology, Fig. 2 reports images of filtered NLD-A (A) and NLD-B (B-D). In the case of NLD-A, only unilamellar vesicles are observed, while unilamellar, bi-lamellar and invaginated vesicles, hexasomes (Fig. 2B), sponge-like structures (Fig. 2C) and cubosomes (Fig. 2D) can be detected in the case of NLD-B. Note that in Figs. 1 and 2 the darker zones refer to lacey carbon film and ice crystals formed during sample preparation. Moreover, it is noteworthy that in the case of NLD-B the presence of CRO promotes hexasome formation.

X-ray diffraction was used to investigate the inner structural organization of NLD. X-ray diffraction profiles were obtained only from NLD before filtration. Experiments were performed both in the presence and in the absence of CRO. Fig. 3 shows the obtained profiles, while Table I summarizes the structural data. For NLD-A, the presence of a 229 (*Im3m*) cubic phase was observed both in the absence and in the presence of CRO, confirming the preservation of the cubosome morphology. Note that unit cell values are very similar, suggesting that the presence of CRO does not alter the lipid structure. In the case of NLD-B, a different behavior was detected: empty NLD-B shows a 229 (*Im3m*) cubic structure (with unit cell similar to those observed in NLD-A), while after the addition of CRO, the presence of an inverted H_{II} hexagonal phase was detected. In this case, CRO induces a transition from the cubosome to hexasome morphology of the nanoparticles.

PCS studies were conducted to determine the dimensional distribution of NLD dispersions after filtration, Table II reports the mean diameters of NLD based on different compositions. Mean diameters expressed as Z Average were comprised between 150 and 250 nm. The addition of sodium caseinate to the mixture monooleine/sodium cholate resulted in a decrease of mean diameter in the case of empty NLD. In both NLD the presence of CRO led to an increase of mean diameter, more emphasized in the case of NLD-B, where the presence of the molecule involved roughly a 90 nm increase. This result is in line with the found nanostructures, indeed in the case of NLD-B, hexasomes formed, leading to an increase of NLD mean diameter. The presence of CRO induced an increase of polydispersity indexes that were always below 0.4.

In order to obtain information about CRO encapsulation and its distribution in the dispersions, after filtration CRO-NLD were treated by ultracentrifugation. The method allowed to evaluate CRO content associated to NLD matrix (disperse phase) and to the aqueous phase (dispersing phase).

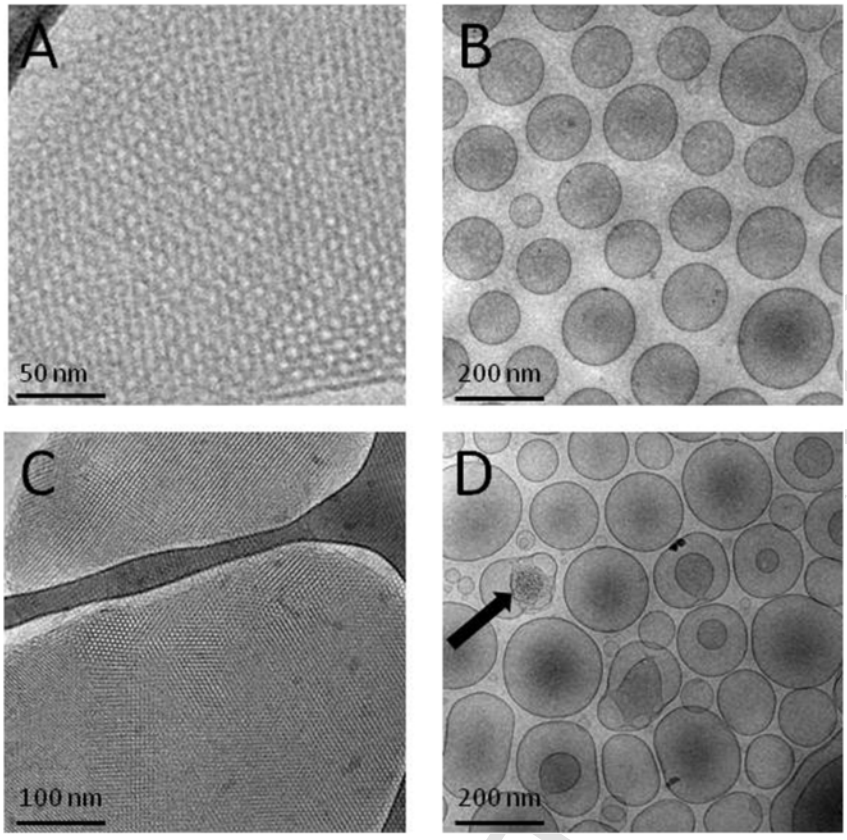

Fig. 1. Cryo-transmission electron microscopy images (cryo-TEM) of empty NLD-A (A, B) and empty NLD-B (C, D) before (A, C) and after (B, D) filtration.

CRO has been encapsulated efficiently in both NLD, with higher EE values in the case of NLD-B (see Table 2). Probably the heterogeneous nanostructures found in this latest type of NLD facilitated the association of CRO on their interface, resulting in higher EE values with respect to the NLD-A, constituted of vesicles. It should be noted that an amount of CRO was dissolved into the aqueous dispersing phase, namely 21.44% and 15.28% for NLD-A and NLD-B respectively. This result is not surprising and can be attributed to the CRO solubility in water.

3.2. In vitro CRO diffusion through SCE membranes

CRO steady state fluxes for the different vehicles are reported in Fig. 4 and Table 3.

CRO fluxes from NLD were lower than from the aqueous solution, namely 2.27 fold in the case of NLD-B and 7.82 fold lower in the case of NLD-A (Table 3). This result indicates that the association of CRO to NLD nanostructures enables to control the rate of drug diffusion through the skin, with respect to the plain aqueous solution.

Statistical analysis revealed significant differences ($p < 0.01$) between fluxes obtained for CRO in aqueous solution and in NLD formulations.

3.3. CRO stability studies

Despite CRO beneficial effects, its poor stability and high susceptibility to process conditions represent major problems for its therapeutic application [19]. Indeed CRO stability is affected by pH, light exposure and temperature.

Firstly the macroscopic aspect of CRO loaded NLD has been evaluated, both maintained yellow colour and almost absence of aggregates, at least after six months from production. Then CRO content in the different formulations has been evaluated as a function of time and expressed as percentage of the total amount used for the preparation (Fig. 5). Remarkably, both NLD were able to longer control CRO stability with respect to CRO water solution, whose half-life is just 3.5 days, as reported in Table 3. Moreover it was found that CRO was more stable in NLD-B with respect to NLD-A, this evidence could be related both to the different supramolecular structures and to pH of NLD. Indeed, in the case of NLD-B, cubic, hexagonal and sponge structures were able to better control CRO stability, with respect to the vesicles present in NLD-A. Moreover, as reported in Table 3, the higher the pH, the higher the CRO stability, as found by other authors [19,20].

3.4. Oxygen radical absorbance assay

The results reported in Fig. 6 showed the antioxidant efficacy of the empty and loaded NLD-A (Fig. 6A) and NLD-B (Fig. 6B) in comparison with CRO alone. The results pointed out that NLD-A (Fig. 6A) after 6 h of incubation was able to preserve the fluorescence of fluorescein (FL) solution with respect to empty NLD-A and CRO solution, quenching the radicals that would have inhibited the fluorescence of FL. A similar trend has been observed with NLD-B (Fig. 6B), although in this case empty NLD-B was able to assurance a certain preservation of fluorescence. This effect was probably due to the presence of sodium caseinate which is reported to possess a good antioxidant activity [21]. CRO solution maintains the same qualitative trend of fluorescence value on both figures, remaining sta-

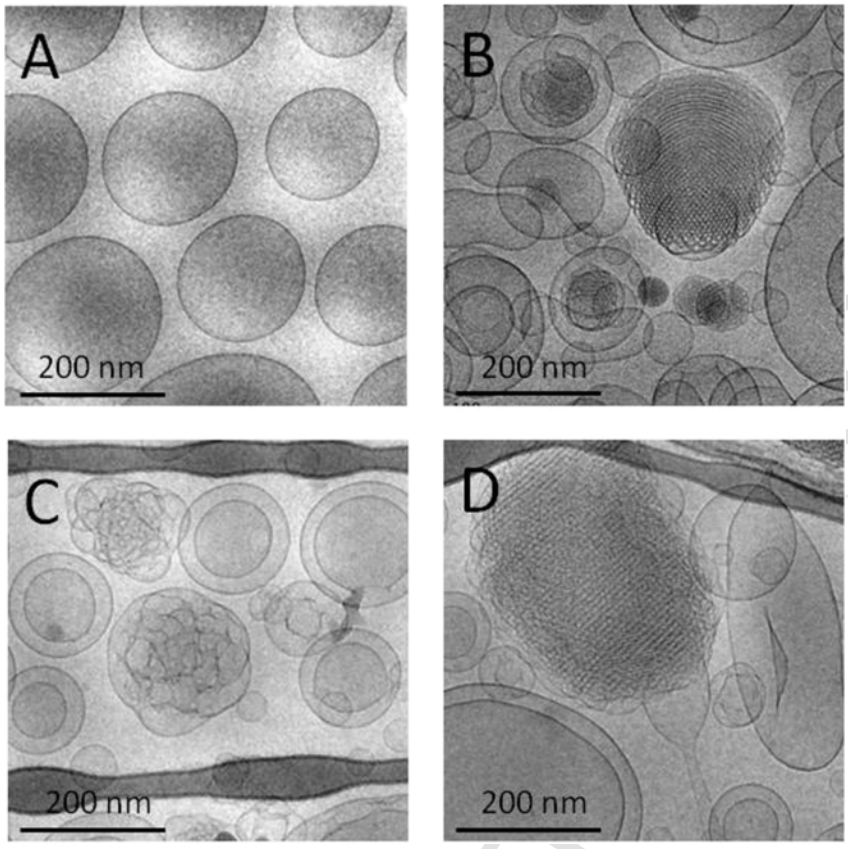

Fig. 2. Cryo-transmission electron microscopy images (cryo-TEM) of filtered NLD-A (panels A) and NLD-B (panels B–D).

ble during the first hours of incubation, while it decays during the remaining period of monitoring, later than NLD-A and NLD-B. Even after 24 h incubation, FL solution containing NLD-A and NLD-B showed high fluorescence compared to empty NLD or the positive control, demonstrating that the antioxidant activity of CRO is maintained for a longer time when it is associated to NLD.

3.5. MTT assay

The results presented in Fig. 7A showed that treatment with plain CRO solution induced a significant decrease of cell viability, whereas both NLD-A and NLD-B inhibited cell proliferation in a higher significant level than plain CRO. MTT assay showed that empty or CRO-loaded vehicles do not interfere with cell viability because they did not reduce the ability of the human fibroblasts, used as a model of normal cells, to metabolize tetrazolium salts (Table 4). Specifically, with respect to untreated cells, a reduction of viability up to 86 + 2% and 90 + 1% was observed after treatment with NLD-A or NLD-B, respectively. With respect to the empty vehicles, the incorporation and the release of CRO was crucial for cell viability, as shown in Fig. 7B.

4. Discussion

Usually researchers employ the commercially available triblock copolymer Pluronic F127 to impart steric stabilization to monoolein based dispersions. Nonetheless, alternative stabilizers based on naturally-occurring constituents can be used to satisfy sustainability requirements. In particular the bile salt sodium cholate and β-casein (the major component of sodium caseinate) [22] are nonsynthetic biocompatible stabilizers able to provide sufficient stabilization to disperse monoolein in excess water [23,24]. The results here presented demonstrate that the choice to employ sodium cholate and sodium caseinate to stabilize the NLD dispersions has been successful.

Cryo-TEM analyses allowed to investigate the internal structures of NLD and to compare the emulsifier influence on the nanostructures of the disperse phase.

The analyses show the obtainment of different nanostructures probably due to the way of association of monoolein with the different stabilizers. Indeed it is well known that bile salts, such as sodium cholate, are able to solubilize polar lipids due to their amphiphilic character in aqueous media [23]. Their peculiar molecular architecture, characterized by a rigid steroid skeleton with a polar surface and an apolar surface instead of the typical structure of traditional surfactants, leads to the formation of lamellar phases in the presence of monoolein [25]. In addition it has been found that the addition of small amounts of sodium cholate to monoolein results in a large swelling of the lipid-based liquid crystalline phase with the consequent formation of a sponge L3 phase [26]. On the other hand the amphiphilic protein casein has a flexible, linear structure, making it an excellent stabilizer of dispersed systems. Indeed β-casein can absorb to the oil-water interface of emulsions, assuming a characteristic interfacial structure that prevents oil particle aggregation through steric stabilization [14]. Different studies have demonstrated that β-casein can self-associate into micellar aggregates in water and it is able to form cubic phases in the presence of monoolein [27,28].

The association of sodium cholate to sodium caseinate in the presence of CRO resulted in an heterogeneous system in which cubic phases coexisted with sponge phases, hexasomes and vesicles. Proba-

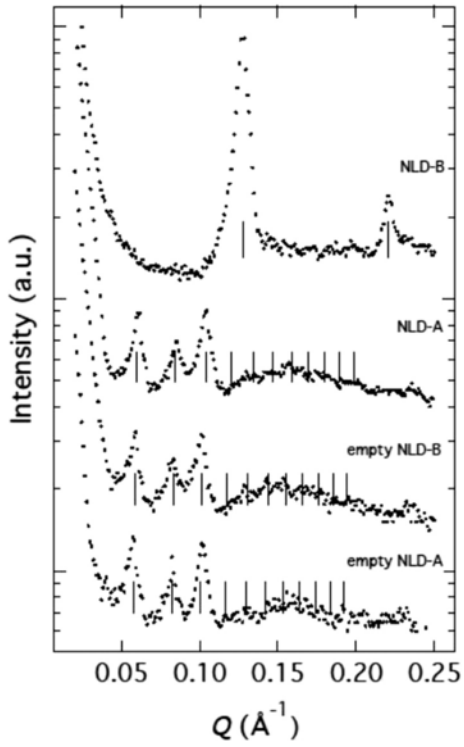

Fig. 3. X-ray diffraction profiles observed on NLD before filtration. From the bottom: empty NLD-A, empty NLD-B, NLD-A and NLD-B. The vertical black lines indicate the expected peak positions: *Im3m*, spacing ratios as √ 2:√4:√6:√8:√10:√12…; H_{II}, spacing ratios as √ 1:√3:√4… $Q = 4\pi \sin\theta / \lambda$, where 2θ is the scattering angle.

Table 2
Dimensional parameters and CRO encapsulation parameters of NLD based on different compositions.

Formulation				
Parameter	Empty NLD-A	NLD-A[a]	Empty NLD-B	NLD-B[a]
ZAverage[b] mean diameter (nm) ± SD	206.8 ± 2.50	230.0 ± 3.0	153.5 ± 1.50	242.0 ± 4.2
Polydispersity index[b] ± SD	0.27 ± 0.02	0.35 ± 0.01	0.29 ± 0.03	0.37 ± 0.02
Encapsulation efficiency[c] (%) ± SD	–	77.06 ± 3.50	–	82.72 ± 1.03
Loading capacity[d] (%) ± SD	–	0.017 ± 0.001	–	0.018 ± 0.001

Data are means of 4 determinations on different batches of the same type of dispersion.

[a] Produced in the presence of crocin.

[b] As determined by PCS.

[c] Percentage (w/w) of CRO in the whole dispersion with respect to the total amount used for the preparation, as determined by ultracentrifugation.

[d] Percentage (w/w) of CRO in the whole dispersion with respect to the amount of lipid used for the preparation.

bly CRO partly interacts with monoolein and emulsifiers, promoting the formation of different crystalline phases.

The results of cryo-TEM observation have been corroborated by X-ray data which were used to investigate the inner structural organization of NLD.

As regards CRO encapsulation, both carriers have guaranteed high EE values. Notably it has been previously demonstrated that NLD are able to solubilize lipophilic molecules, such as indomethacin, curcumin and bromocriptine [13,14,17], by encapsulation in the disperse phase. Instead, in the present investigation we have demonstrated that also hydrophilic molecules, such as CRO, can be efficiently solubilized into NLD, associating in a different extent within the disperse and the dispersing phase.

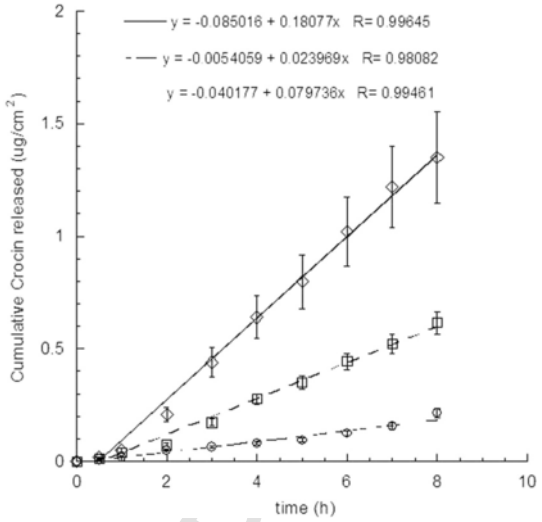

Fig. 4. CRO permeability profiles from aqueous solution (diamonds), NLD-A (circles) and NLD-B (squares), as determined by Franz cell associated to SCE membranes. Data represent the mean of 4 independent experiments ± S.D.

Table 3
pH, flux values and half life periods of CRO contained in different vehicles.

Vehicles	pH	Flux (cm/h × 10^3)	Half life (days)
Water	6.18 ± 0.02	0.180 ± 0.07	3.5 ± 0.1
NLD-A[a]	7.48 ± 0.01	0.023 ± 0.03	42.3 ± 0.2
NLD-B[a]	8.08 ± 0.02	0.079 ± 0.02	52.7 ± 0.4

Data represent the mean of 4 independent experiments ± S.D.
Vehicles were stored at 25 °C.

[a] NLD produced in the presence of CRO.

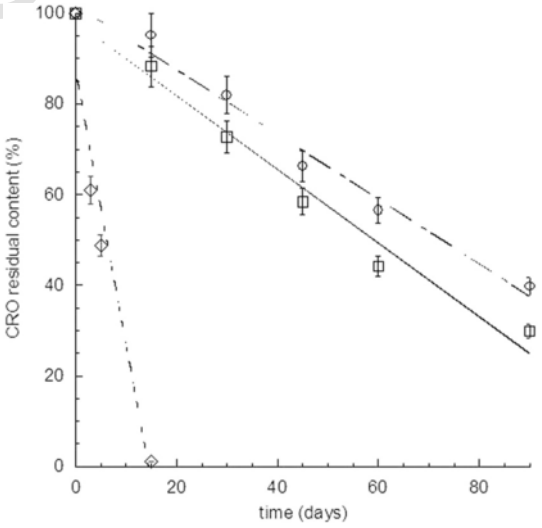

Fig. 5. CRO content in aqueous solution (diamonds), NLD-A (circles) and NLD-B (squares), as a function of time. Chemical stability was evaluated on filtered drug loaded formulations, stored at 25 °C in the dark for 3 months, determining CRO content by HPLC analyses. Data are the means of 4 analyses on different batches of the same type of dispersions.

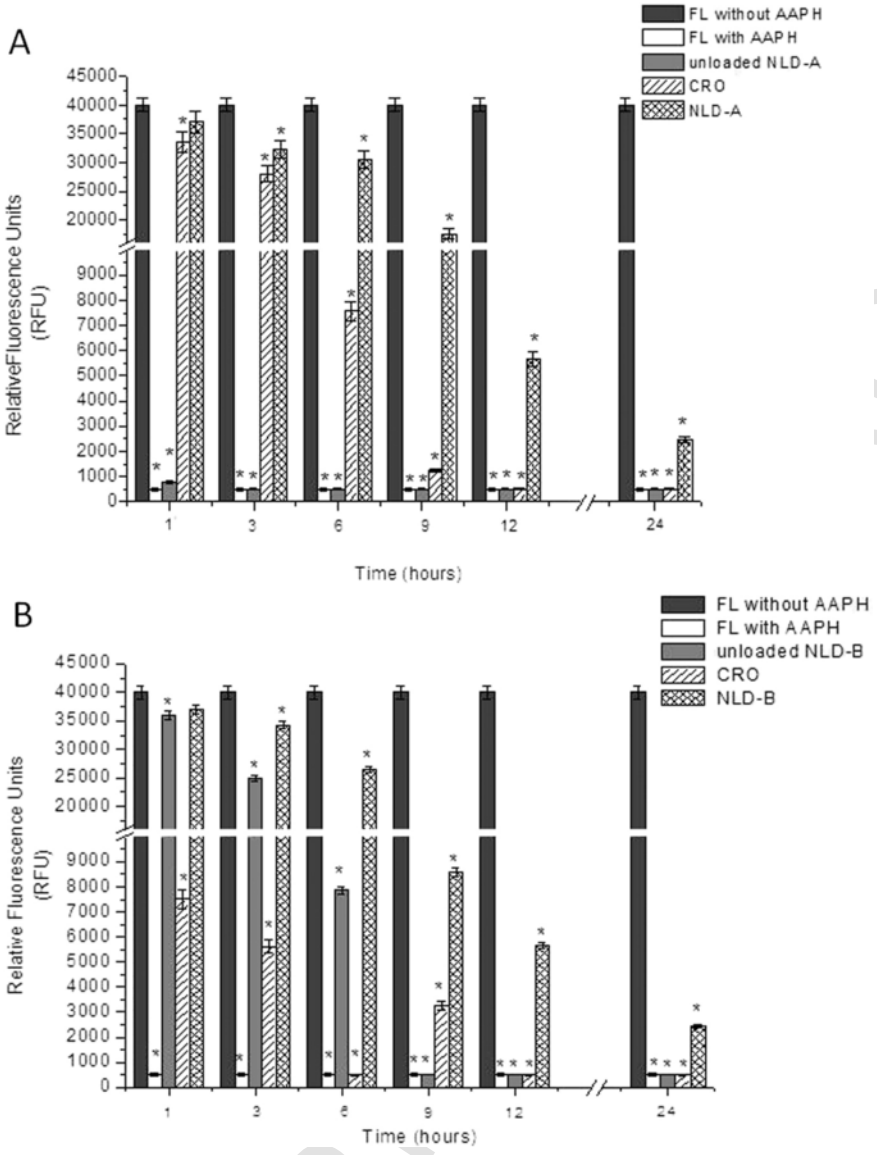

Fig. 6. ORAC assays for NLD-A (panel A) and NLD-B (panel B). Data represent the mean of three independent experiments ± S.D.. *p < 0.05.

The in vitro CRO diffusion through SCE membranes was studied in order to investigate the efficiency of NLD designed as topical cutaneous vehicles.

The results indicate that NLD nanostructures were able to control the rate of CRO diffusion through the skin, with respect to the control formulation. Interestingly, CRO diffused faster from NLD-B than from NLD-A. These different fluxes could be attributed to the heterogeneous structures in the former dispersion, constituted of cubosomes, hexasomes, sponge systems and vesicles. Indeed it has been demonstrated that formulations with the same lipid composition but different self-assembly differently interact with *stratum corneum* [29,30]. For instance in the case of vesicles, the lipid bilayer could mix with the lipid channel within the intercellular spaces between the horny cells, leading to the formation of a depot system that controls drug diffusion through the skin [31].

With regard to cubosome and hexasome contribution, it should be considered that some authors have detected a similarity between the cubic phase structure and the structure of the *stratum corneum* [32]. Indeed, according to the cubic rod-packing and membrane templating model of epidermal keratin structure and formation, it is recognized that the epidermal barrier organization presupposes an energetically favorable transition from cubic to lamellar phase [33]. This theory presumes the presence of keratin intermediate filaments in the different strata of the epidermis in hexagonal and cubic forms. Thus exogenous cubic or hexagonal phases applied on skin could seamlessly integrate with the endogenous biological cubic architecture of keratin.

In this view, the contribution given by cubic, hexagonal and sponge phases in the case of NLD-B could lead to a more efficacious interaction with SCE membranes with respect to NLD-A, characterized by the only presence of vesicles that possibly form a reservoir within the lamellar bilayers of the *stratum corneum*. Finally, the merging of NLD-B nanostructures with SCE should result in a higher CRO flux with respect to NLD-A.

The antioxidant potential of NLD has been evaluated by means of an ORAC assay. In particular this test measures antioxidant inhibition of peroxyl radical induced oxidation and thus reflects classical radical chain breaking antioxidant activity by H atom transfer.

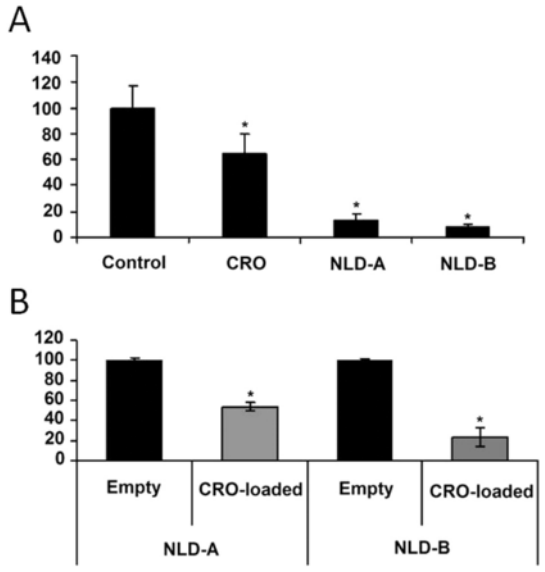

Fig. 7. Antiproliferative activity of NLD-A and NLD-B against a human melanoma cell line (A375): versus CRO solution in PBS, (0.1% w/w) (panel A) and versus empty NLD (panel B). Each value represents the mean ± SD of three experiments, performed in duplicate. * significant vs. control untreated cells ($p < 0.05$).

Table 4
Cell viability of normal human adult fibroblasts treated with NLD.

Vehicles	Cell viability % compared to untreated controls
Control	100
Empty NLD-A	98 ± 1.6
NLD-A	96 ± 2.3
Empty NLD-B	99 ± 3.1
NLD-B	96 ± 4.1

Data represent the mean of 3 independent experiments ± S.D.
Vehicles were stored at 25 °C.

Our studies clearly show the NLD capability to maintain or prolong CRO antioxidant activity. This result is probably related to the protective effect of NLD, able on one hand to preserve CRO from instability phenomena and on the other to release the drug in a controlled fashion.

The assessment of NLD-A or NLD-B as biocompatible vehicles for CRO delivery was achieved thanks to biological experiments performed by using a human melanoma cell line. To evaluate the capability of NLD-A and NLD-B to release CRO within the cell compartment and block cellular proliferation, the cells were incubated with treatment medium in the presence of CRO solution, NLD-A or NLD-B. Under these conditions, cell viability experiments were performed. The obtained results are in line with previous in vitro studies showing antiproliferative effect of CRO in various tumor cell lines [34,35], furthermore the obtained data emphasize the role of NLD as vehicles potentiating CRO anticancer activity. Probably this enhanced activity is due to an increased CRO stability following its incorporation in NLD.

5. Conclusions

This work has suggested a new strategy to vehiculate the antioxidant CRO and to protect the molecule from degradation.

In particular Franz cell studies and stability tests showed that NLD-B is able to promote CRO diffusion through SCE and to better control CRO degradation with respect to NLD-A.

Furthermore, ORAC assay pointed out an interesting and prolonged antioxidant activity of CRO once vehiculated by NLD, while an in vitro MTT test, performed on a human melanoma cell line, showed an increase of CRO antiproliferative effect after incorporation in NLD. These results could be attributed to NLD protective effect against CRO chemical hydrolysis and photo instability phenomena.

CRO containing NLD could be possibly proposed as vehicles for topical administration of the molecule, nonetheless in vivo studies will be required to confirm this hypothesis.

Acknowledgements

This work was funded by "FIRB 2010 Fondo per gli Investimenti della Ricerca di Base" from the Ministry of the University and Research of Italy (code RBFR10XKHS).

Appendix A. Supplementary data

Supplementary data to this article can be found online at doi:10.1016/j.msec.2016.10.045.

References

[1] P. Winterhalter, R.M. Straubinger, Saffron, Renewed interest in an ancient spice, Food Rev. Intl. 16 (2000) 39–59.
[2] R. Rezaee, H. Hosseinzadeh, Safranal: from an aromatic natural product to a rewarding pharmacological agent, Iran. J. Basic Med. Sci. 16 (2013) 12–26.
[3] F.I. Abdullaev, J.J. Espinosa-Aguirre, Biomedical properties of saffron and its potential use in cancer therapy and chemoprevention trials, Cancer Detect. Prev. 28 (2004) 426–432.
[4] S.H. Alavizadeh, H. Hosseinzadeh, Bioactivity assessment and toxicity of crocin: a comprehensive review, Food Chem. Toxicol. 64 (2014) 65–80.
[5] J. Escribano, G.L. Alonso, M. Coca-Prados, J.A. Fernandez, Crocin, safranal and picrocrocin from saffron (Crocus sativus L.) inhibit the growth of human cancer cells in vitro, Cancer Lett. 100 (1996) 22–30.
[6] T. Konoshima, M. Takasaki, H. Tokuda, S. Morimoto, H. Tanaka, E. Kawata, L.J. Xuan, H. Saito, M. Sugiura, J. Molnar, Y. Shoyama, Crocin and crocetin derivatives inhibit skin tumor promotion in mice, Phytother. Res. 12 (1998) 400–404.
[7] D. Hanahan, R.A. Weinberg, The hallmarks of cancer, Cell 100 (2000) 57–70.
[8] S. Rakoff-Nahoum, Why cancer and inflammation?, Yale J. Biol. Med. 79 (2006) 123–130.
[9] J. Marnewick, E. Joubert, S. Joseph, S. Swanevelder, P. Swart, W. Gelderblom, Inhibition of tumor promotion in mouse skin by extracts of rooibos (Aspalathus linearis) and honeybush (Cyclopia intermedia), unique south African herbal teas, Cancer Lett. 224 (2005) 193–202.
[10] M. Tsimidou, E. Tsatsaroni, Stability of saffron pigments in aqueous extracts, J. Food Sci. 58 (1993) 1073–1075.
[11] B. Siekmann, H. Bunjes, M.H.J. Koch, K. Westesen, Preparation and structural investigations of colloidal dispersions prepared from cubic monoglyceride/water phases, Int. J. Pharm. 244 (2002) 33–43.
[12] A. Yaghmur, O. Glatter, Characterization and potential applications of nanostructured aqueous dispersions, Adv. Colloid Interf. Sci. 147 (2009) 333–342.
[13] C. Puglia, V. Cardile, A.M. Panico, L. Crascì, A. Offerta, S. Caggia, M. Drechsler, P. Mariani, R. Cortesi, E. Esposito, Evaluation of monoolein aqueous dispersions as tools for topical administration of curcumin: characterization, in vitro and ex-vivo studies, J. Pharm. Sci. 102 (2011) 2349–2361.
[14] E. Esposito, P. Mariani, L. Ravani, C. Contado, M. Volta, S. Bido, M. Drechsler, S. Mazzoni, E. Menegatti, M. Morari, R. Cortesi, Nanoparticulate lipid dispersions for bromocriptine delivery: characterization and in vivo study, Eur. J. Pharm. Biopharm. 80 (2012) 306–314.
[15] R. Pecora, Dynamic light scattering measurement of nanometer particles in liquids, J. Nanopart. Res. 2 (2000) 123–131.
[16] A.P. Nayak, W. Tiyaboonchai, S. Patankar, B. Madhusudhan, E.B. Souto, Curcuminoids loaded lipid nanoparticles: novel approach towards malaria treatment, Colloids Surf. B 81 (2010) 263–273.
[17] E. Esposito, R. Cortesi, M. Drechsler, L. Paccamiccio, P. Mariani, C. Contado, E. Stellin, E. Menegatti, F. Bonina, C. Puglia, Cubosome dispersions as delivery systems for percutaneous administration of indomethacin, Pharm. Res. 22 (2005) 2163–2173.
[18] J.G. Merrell, S.W. McLaughlin, L. Tie, C.T. Laurencin, A.F. Chen, L.S. Nair, Curcumin-loaded poly(epsilon-caprolactone) nanofibres: diabetic wound dress-

ing with anti-oxidant and anti-inflammatory properties, Clin. Exp. Pharmacol. Physiol. 36 (2009) 1149–1156.
[19] S. Rahaiee, S.A. Shojaosadati, M. Hashemi, S. Moini, S.H. Razavi, Improvement of crocin stability by biodegradeble nanoparticles of chitosan-alginate, Int. J. Biol. Macromol. 79 (2015) 423–432.
[20] Z.-T. Wang, X. Fu, An investigation into the stability of crocin-1, Food Sci. 33 (2012) 71–73.
[21] S.P. O'Dwyer, D. O'Beirne, D.N. Eidhin, B.T. O'Kennedy, Effects of sodium caseinate concentration and storage conditions on the oxidative stability of oil-in-water emulsions, Food Chem. 138 (2013) 1145–1152.
[22] N.C. Woodward, A.P. Gunning, A.R. Mackie, P.J. Wilde, V.J. Morris, Comparison of the orogenic displacement of sodium caseinate with the caseins from the air − water interface by nonionic surfactants, Langmuir 25 (2009) 6739–6744.
[23] M. Lindstrom, H. Ljusberg-Wahren, K. Larsson, B. Borgstrom, Aqueous lipid phases of relevance to intestinal fat digestion and absorption, Lipids 16 (1981) 749–754.
[24] M. Golding, A. Sein, Surface rheology of aqueous casein-monoglyceride dispersions, Food Hydrocoll. 18 (2004) 451–461.
[25] J. Gustafsson, T. Nylander, M. Almgren, H. Ljusberg-Wahren, Phase behavior and aggregate structure in aqueous mixtures of sodium cholate and glycerol monooleate, J. Colloid Interface Sci. 211 (1999) 326–335.
[26] C.V. Kulkarni, Lipid crystallization: from self-assembly to hierarchical and biological ordering, Nanoscale 4 (2012) 5779–5791.
[27] J. Zhai, L. Waddington, T.J. Wooster, M.I. Aguilar, B.J. Boyd, Revisiting β-casein as a stabilizer for lipid liquid crystalline nanostructured particles, Langmuir 27 (2011) 14757–14766.
[28] I. Portnaya, R. Khalfin, E. Kesselman, O. Ramon, U. Cogan, D. Danino, Mixed micellization between natural and synthetic block copolymers: β-casein and Lutrol F-127, Phys. Chem. Chem. Phys. 13 (2011) 3153–3160.
[29] L. Barbosa-Barros, C. Barba, G. Rodriguez, M. Cocera, L. Coderch, C. Lopez-Iglesias, A. De La Maza, O. Lopez, Lipid nanostructures: self-assembly and effect on skin properties, Mol. Pharm. 6 (2009) 1237–1245.
[30] M. Foldvari, I. Badea, S. Wettig, D. Baboolal, P. Kumar, A.L. Creagh, C.A. Haynes, Topical delivery of interferon alpha by biphasic vesicles: evidence for a novel nanopathway across the stratum corneum, Mol. Pharm. 7 (2010) 751–762.
[31] C. Puglia, F. Bonina, L. Rizza, R. Cortesi, E. Merlotti, M. Drechsler, P. Mariani, C. Contado, L. Ravani, E. Esposito, Evaluation of percutaneous absorption of naproxen from different liposomal formulations, J. Pharm. Sci. 99 (2010) 2819–2829.
[32] N. Lars, A.-A. Ashraf, Stratum corneum keratin structure, function, and formation: the cubic rod-packing and membrane templating model, J. Investig. Dermatol. 4 (2004) 715–732.
[33] S. Hoath, L. Norlen, Cubic phases and human skin: theory and practice, in: M.L. Lynch, P.T. Spicer (Eds.), Bicontinuous Liquid Crystals, CRC Press Taylor and Francis Group, Boca Raton, FL, 2005, pp. 41–58.
[34] C. Festuccia, A. Mancini, G.L. Gravina, L. Scarsella, S. Llorens, G.L. Alonso, C. Tatone, E. Di Cesare, E.A. Jannini, A. Lenzi, A.M. D'Alessandro, M. Carmona, Antitumor effects of saffron-derived carotenoids in prostate cancer cell models, Biomed. Res. Int. 2014 (2014) 135048.
[35] S.H. Kim, J.M. Lee, S.C. Kim, C.B. Park, P.C. Lee, Proposed cytotoxic mechanisms of the saffron carotenoids crocin and crocetin on cancer cell lines, Biochem. Cell Biol. 92 (2014) 105–111.